PWT FILE COPY

AEDC-TR-80-60

P32A-K9A

Captive Aircraft Testing at High Angles of Attack

R. W. Butler and J. P. Christopher
ARO, Inc.

August 1981

Final Report for Period October 1976 – September 1978

ARNOLD ENGINEERING DEVELOPMENT CENTER
ARNOLD AIR FORCE STATION, TENNESSEE
AIR FORCE SYSTEMS COMMAND
UNITED STATES AIR FORCE

NOTICES

When U. S. Government drawings, specifications, or other data are used for any purpose other than a definitely related Government procurement operation, the Government thereby incurs no responsibility nor any obligation whatsoever, and the fact that the Government may have formulated, furnished, or in any way supplied the said drawings, specifications, or other data, is not to be regarded by implication or otherwise, or in any manner licensing the holder or any other person or corporation, or conveying any rights or permission to manufacture, use, or sell any patented invention that may in any way be related thereto.

Qualified users may obtain copies of this report from the Defense Technical Information Center.

References to named commercial products in this report are not to be considered in any sense as an indorsement of the product by the United States Air Force or the Government.

This report has been reviewed by the Office of Public Affairs (PA) and is releasable to the National Technical Information Service (NTIS). At NTIS, it will be available to the general public, including foreign nations.

APPROVAL STATEMENT

This report has been reviewed and approved.

Alexander F. Money

ALEXANDER F. MONEY
Directorate of Technology
Deputy for Operations

Approved for publication:

FOR THE COMMANDER

Marion L. Laster

MARION L. LASTER
Director of Technology
Deputy for Operations

REPORT DOCUMENTATION PAGE		READ INSTRUCTIONS BEFORE COMPLETING FORM
1. REPORT NUMBER AEDC-TR-80-60	2. GOVT ACCESSION NO.	3. RECIPIENT'S CATALOG NUMBER
4. TITLE (and Subtitle) CAPTIVE AIRCRAFT TESTING AT HIGH ANGLES OF ATTACK		5. TYPE OF REPORT & PERIOD COVERED Final Report, October 1976 to September 1978
		6. PERFORMING ORG. REPORT NUMBER
7. AUTHOR(s) R. W. Butler and J. P. Christopher, ARO, Inc., a Sverdrup Corporation Company		8. CONTRACT OR GRANT NUMBER(s) -
9. PERFORMING ORGANIZATION NAME AND ADDRESS Arnold Engineering Development Center/DOT Air Force Systems Command Arnold Air Force Station, Tennessee 37389		10. PROGRAM ELEMENT, PROJECT, TASK AREA & WORK UNIT NUMBERS Program Element 65807F
11. CONTROLLING OFFICE NAME AND ADDRESS Arnold Engineering Development Center/DOS Air Force Systems Command Arnold Air Force Station, Tennessee 37389		12. REPORT DATE August 1981
		13. NUMBER OF PAGES 44
14. MONITORING AGENCY NAME & ADDRESS(if different from Controlling Office)		15. SECURITY CLASS. (of this report) UNCLASSIFIED
		15a. DECLASSIFICATION/DOWNGRADING SCHEDULE N/A

16. DISTRIBUTION STATEMENT (of this Report)

Approved for public release; distribution unlimited.

17. DISTRIBUTION STATEMENT (of the abstract entered in Block 20, if different from Report)

18. SUPPLEMENTARY NOTES

Available in Defense Technical Information Center (DTIC).

19. KEY WORDS (Continue on reverse side if necessary and identify by block number)

wind tunnel tests
wind tunnel models
angle of attack
maneuverability
captive flight
captive tests
computer applications

20. ABSTRACT (Continue on reverse side if necessary and identify by block number)

A captive testing technique capable of simulating aircraft maneuvers at high angles of attack has been developed and tested in the Aerodynamic Tunnel 16T of the Arnold Engineering Development Center (AEDC). The captive technique uses a closed loop system between wind tunnel, model, and computer. Use of the wind tunnel as an analog forcing function eliminates the requirement for a conventional static data matrix in motion simulation. Various high

DD FORM 1 JAN 73 1473 EDITION OF 1 NOV 65 IS OBSOLETE

20. ABSTRACT, Concluded.

angle-of-attack maneuvers (rudder roll, aileron roll, wind-up turn, etc.) were generated with the captive system and show good correlation with flight data.

AFSC
Arnold AFS Tenn

PREFACE

The work reported herein was conducted by the Arnold Engineering Development Center (AEDC), Air Force Systems Command (AFSC). The results of the research were obtained by ARO, Inc., AEDC Group (a Sverdrup Corporation Company), operating contractor for the AEDC, AFSC, Arnold Air Force Station, Tennessee, under ARO Project Number P32A-K9A. The Air Force project manager was Mr. A. F. Money, AEDC/DOT. The manuscript was submitted for publication on October 13, 1980.

Messrs. R. W. Butler and J. P. Christopher are currently employed by Calspan Field Services, Inc., AEDC Division.

CONTENTS

ILLUSTRATIONS

TABLE

Page

APPENDIXES

1.0 INTRODUCTION

During the past five years a number of experiments have been conducted at the Arnold Engineering Development Center (AEDC) for determining the feasibility of simulating aircraft motion in the wind tunnel. This motion simulation technique is referred to as Captive Aircraft Testing. With this type of testing aircraft maneuvers may be simulated in the wind tunnel without the need of the conventional complex and costly static data matrices. The wind tunnel acts as the static analog forcing function, providing an infinite static data matrix which is independent of model configuration. Maneuver limitations are purely a function of wind tunnel model-positioning hardware (support travel) and model-associated hardware (remote control surfaces). With the captive testing tool experimentalists may examine the flight characteristics of aircraft in a more accurate and efficient manner than heretofore possible through conventional motion simulation techniques.

Evolution of Captive Aircraft Testing at AEDC is documented in Refs. 1, 2, and 3. The initial system development and checkout (Ref. 2) were conducted as a pilot test in the AEDC Aerodynamic Wind Tunnel (4T) using an A-7 aircraft model with fixed control surfaces. The success of the 4T experiment led to a series of additional tests (Ref. 3) in the AEDC Propulsion Wind Tunnel (16T). These later 16T experiments utilized an F-15 aircraft model with remote control horizontal stabilizers which provided the capability of simulating aircraft maneuvers in the longitudinal plane. Correlation of the F-15 longitudinal captive generated motion with flight test data was excellent.

Due to the success of the above experimental captive programs a new 16T captive system oriented toward user testing has recently been developed. The new system is designed for an aircraft model with a full complement of aerodynamic controls (rudder, elevator, and aileron). In addition, computer software used in tunnel/computer interfaces has been simplified to make feasible the use of the captive system on a routine basis.

Documentation of the capabilities and validity of the captive system is accomplished with direct comparisons of F-15 captive versus flight motion. Complex longitudinal and lateral/directional high angle-of-attack (AOA) maneuvers are utilized in the documentation. These wind tunnel/flight data comparisons, along with other work accomplished during system development, are reported herein.

2.0 APPARATUS

2.1 TEST FACILITY

The AEDC Propulsion Wind Tunnel (16T) is a variable density, continuous flow tunnel capable of being operated at Mach numbers from 0.2 to 1.6 and stagnation pressures from 120 to 4,000 psfa. The maximum attainable Mach number can vary slightly depending upon the tunnel pressure ratio requirements with a particular test installation. The maximum stagnation pressure attainable is a function of Mach number and available electrical power. The tunnel stagnation temperature can be varied from about 80 to 160°F, depending upon the available cooling water temperature. The test section is 16 ft square by 40 ft long and is enclosed by 60-deg inclined-hole perforated walls of six-percent porosity. Additional information about the tunnel, its capabilities, and operating characteristics is presented in Ref. 4.

2.2 TEST CONDITIONS

Captive tests were conducted at M_∞ = 0.3 to 0.9 at corresponding total pressure levels from 2,000 to 1,000 psf, respectively. Within this Mach number and total pressure range the model Reynolds number, based on the wing mean aerodynamic chord, ranged from 1.6 to 1.9 x 10^6. Flow angularity corrections were applied to both angle of attack and sideslip as a function of Mach number. Model blockage corrections were not considered to be important in this test due to the low ratio of model to tunnel cross-sectional area (approximately 1 percent at 90 deg AOA).

2.3 MODEL DESCRIPTION

The aircraft model used in this captive testing was a rigid (all steel) 1/20-scale F-15. Basic dimensions of the model are shown in Fig. 1. The model was equipped with production snag stabilators and raked wingtips. Engine inlets were maintained in the drooped configuration, nose down, representative of the F-15 high-AOA flight configuration. The inlets were plugged just inside the inlet lip, by a flat plate normal to the duct. The model installed in the Tunnel 16T test section is shown in Fig. 2.

Primary aerodynamic control surfaces (horizontal stabilizers, rudders, and ailerons) of the F-15 were incorporated in the wind tunnel model. The surfaces were remotely controlled and movable over the full range of the production aircraft (horizontal stabilizer + 15 to -25 deg, ailerons ± 20 deg, and rudders ± 30 deg). The horizontal stabilizers could be operated

both differentially and simultaneously. Control surface positions were obtained directly from the surface through a strain-gage/flexure arrangement as shown for the aileron in Fig. 3. The direct readout minimized the hysteresis and general looseness often occuring in mechanical control surface readouts. Also shown in Fig. 3 is the unique aileron drive system developed at AEDC for obtaining remote aileron control on small models with thin wings. The system is designed around a rhombus with a screw jack actuation. The flex cable actuating the screw jack is driven by a servo housed in the wing root region. The overall performance of the system was good during the course of testing.

It should be noted that the wind tunnel model used in testing was tailored to the F-15 production aircraft. F-15 flight test data presented in Section 4.0 of this report are for an F-15 aircraft modified for high-AOA testing. The differences between the wind tunnel model and the modified flight test aircraft are as follows: (1) a spin recovery chute was installed on the flight test aircraft, slightly altering the fuselage afterbody; (2) the mass balance booms on the vertical tail of the flight test aircraft were removed; and (3) the flight test aircraft utilized a test noseboom with flow indicators (vanes) for monitoring angle of attack and sideslip.

3.0 PROCEDURE

3.1 CAPTIVE MOTION SIMULATION

Captive testing is accomplished using a closed loop system of model, wind tunnel, and digital computers as shown in Fig. 4. The wind tunnel model is installed on a six-component internal strain-gage balance which provides static forces and moments. The tunnel acts as an analog forcing function to the model and also provides the AOA and angle of sideslip envelope shown in Fig. 5 via the model-positioning system. Online digital computers control tunnel/model hardware and perform calculations required for conducting motion simulation.

Normally the model is positioned in the tunnel at some trimmed AOA and sideslip angle for a specific flight condition. Upon initiation of the maneuver, appropriate model control surfaces are deflected and static forces and moments are measured. The static aerodynamic measurements are input to an online digital computer where corrections for aircraft flexibility, tunnel flow angularities, etc. are applied. These static aerodynamics are now combined with additional external forces (dynamic and thrust characteristics) and are used in solving the Euler equations of motion presented in Appendix A. The computed solutions to the Euler equations are used in controlling the orientation of the model through a point

prediction technique. The technique involves using the last two successive measured values of each static aerodynamic coefficient to predict the magnitude of the coefficient over the next prediction interval. The prediction interval used in the subject test was 0.05 sec. The predicted coefficients are used to calculate the new model AOA and sideslip by integrating the equations of motion every 0.005 sec over the prediction interval. The model-positioning system is then commanded to move the model to the new angles, where the static aerodynamic forces and moments are remeasured. The above process is repeated until a complete maneuver is generated.

The aircraft Mach number is calculated at each prediction interval, and the wind tunnel Mach number is adjusted to within ± 0.003 of the calculated value. Thus, the aerodynamic coefficients are measured at the correct Mach number throughout the maneuver. Also, the aircraft thrust is calculated and modified with each prediction interval by mathematically modeling the simulated aircraft engine/inlet installed thrust as a function of Mach number, altitude, angle of attack, and angle of sideslip.

Specific maneuvers are programmed through the aircraft flight control system. Normally longitudinal and lateral stick position and rudder pedal position as a function of time are the inputs used in simulating maneuvers. As an option the control surface deflections may be programmed directly, thereby bypassing the aircraft flight control system. For this test the F-15 flight control system (including the control Augmentation System, AS) was modeled and utilized as presented in Appendix B.

3.2 PRECISION OF DATA

Maneuvers generated using the captive technique are subject to error from several sources including tunnel conditions, the angle-positioning system, balance measurements, and extrapolation tolerances allowed in the predicted coefficients. The uncertainties (combinations of systematic and random errors) in the basic tunnel parameters are shown in Fig. 6. These data were estimated from repeat calibration of instrumentation and from the repeatability and uniformity of the test section flow during tunnel calibration. Uncertainties in the instrumentation systems were estimated from repeat calibration of the systems against secondary standards whose uncertainties are traceable to the National Bureau of Standards calibration equipment. The instrument uncertainties are combined using the Taylor series method of error propagation described in Ref. 5 to determine the uncertainties of the reduced parameters.

The maximum uncertainty in the model-positioning system was ± 0.1 deg for settings in AOA and angle of sideslip. Based on the above uncertainties and those resulting from

balance inaccuracies and coefficient prediction tolerances, it is estimated that over the maneuver time span presented the maximum error occurring in the angular position data, θ, ψ, and ϕ will be less than ± 1 deg. These estimates were calculated from the following equations, which assume no inertia or aerodynamic coupling.

$$\ddot{\theta} = \frac{\Delta M_y}{I_y} \qquad \ddot{\psi} = \frac{\Delta M_z}{I_z} \qquad \ddot{\phi} = \frac{\Delta M_x}{I_x}$$

4.0 RESULTS AND DISCUSSION

4.1 GENERAL

The usefulness and validity of a new wind tunnel testing technique such as Captive Aircraft Testing can best be ascertained through comparisons with flight test data. The flight test data used in this report were obtained from the F-15A approach-to-stall/stall/post-stall program (Ref. 6) conducted at the Air Force Flight Test Center. This flight program was selected because it encompasses most of the high-AOA maneuver capability of modern fighter aircraft. The wind tunnel simulation of these high-AOA maneuvers will provide a rigid check on the captive testing systems capabilities. The validity of the captive system for less demanding, low-AOA maneuvers has been previously demonstrated (Ref. 3).

As in conventional aircraft motion simulation, the wind tunnel-measured external rigid forces and moments in captive testing were corrected for airframe flexibility. These corrections were modeled as functions of Mach number, altitude, angle of attack, and load factor. The flexibility math model was formulated with assistance from both the F-15 airframe manufacturer and the Air Force F-15 System Projects Office (SPO). Due to its complexity, the flexibility model is not included herein. In addition to flexibility corrections, the aircraft measured pitching moment (C_m) was adjusted for inlet rotation (previous wind tunnel tests have shown C_m to be a function of inlet angle). Inlet angle on the flight vehicle is scheduled as a function of angle of attack; therefore, corrections to C_m were included when the model fixed inlet angle of 11 deg did not correspond to the scheduled angle.

Dynamic characteristics of the F-15 aircraft were included in the simulation as a math model. The dynamic data utilized were formulated from wind tunnel, flight, and analytical predictions. Their validity may be justified only from the fact that in previous motion simulation studies they produced reasonable results. The dynamic data matrix was formulated with inputs received from both the F-15 airframe manufacturer and the SPO.

As previously noted in Section 3.1, the aircraft flight control system (including control augmentation system) as modeled in this experiment is presented in Appendix B.

Simplifications in the control system incorporated for captive testing were: (1) flight was limited to subsonic conditions, (2) all time constants less than 0.05 sec were omitted, and (3) mechanical inputs were limited to stick and rudder positions (i.e., stick dynamics were not included).

The aircraft mass, inertia, and cg position simulated in the captive generated maneuvers are identical to those for corresponding flight maneuvers in Ref. 1. Table 1 lists these parameters for the simulated manuevers included herein.

4.2 LATERAL/DIRECTIONAL COMMANDED MOTION

Captive maneuvers generated in the lateral and directional planes of motion are presented for comparison with flight motion in this section. Because of their simplicity the F-15 full lateral stick roll (Fig. 7) and full rudder pedal roll (Fig. 8) were selected for initial comparison. These maneuvers are considered simple from a motion simulation viewpoint because they occur at aircraft angles of attack below stall (10 to 20 deg) and are for the most part commanded motion resulting from control surface deflections (aileron and rudder). The full lateral stick roll motion presented in Fig. 7 is in good agreement with flight data. The lateral/directional parameter roll rate (p), yaw rate (r), and roll angle (PHI) are near-overlays of the flight data. Small discrepancies occurring in pitch rate (q) may be attributed to small horizontal stabilizer movements which were not modeled in the captive system via the longitudinal stick input. The full rudder pedal roll of Fig. 8 also shows good agreement between captive and flight motion. Again, the small differences occurring in the longitudinal and directional motion rates may be attributed to discrepancies in modeling of the longitudinal stick and rudder pedal.

The rate of data acquisition experienced in generating the captive motion of Figs. 7 and 8 was 3.0 to 3.5 min of wind tunnel time per 1 sec of flight time. The limiting factor was positioning of the model control surfaces. The 3.5 min/sec rate should be considered typical for maneuvers possessing large control deflection rates.

A hidden attribute in captive testing which often plays a significant part in accurate motion simulation is the inherent modeling of control surface interactions (rudder, horizontal stabilizer, etc.). For control surfaces in close proximity which experience large deflections, as in Fig. 8, interactions often become significant and thereby affect vehicle aerodynamics. Conventional motion simulation cannot sufficiently account for such interactions because of the requirement for unrealistically large data matrices and corresponding wind tunnel programs.

4.3 WINGS-LEVEL STALLS

One of the first high angle-of-attack maneuvers flown in most flight test programs is the 1-"g" stall. Although this maneuver is normally considered simple in the flight program, it sometimes causes problems when one attempts to reproduce it via motion simulation. The problem area is associated with uncommanded lateral/directional motion occurring at high angles of attack. This motion may be seen in Fig. 9, where lateral/directional parameters Beta, P, and R become oscillatory while both lateral stick and rudder pedal are fixed. The oscillatory motion is believed to result from separated and asymmetric flow over the aircraft resulting in nonlinear and hysteresis effects in the aircraft aerodynamics. Unless these aerodynamic phenomena are both defined and modeled properly in the data matrices of motion programs, the chances of simulating these uncommanded motions are poor. As seen in Fig. 9, the captive system does a good job of simulating these motions as a result of inherently accounting for nonlinear and hysteresis effects. The fact that the motion is approximately 90 deg out of phase is insignificant since the onset of the excitation (flow separation) is not always predictable.

An abrupt or more accelerated wings-level stall is shown in Fig. 10. As observed in the 1-"g" stall the uncommanded lateral/ directional motion (wing rock) commences in the 20-to 25-deg angle-of-attack range. An improvement in the onset of the uncommanded motion is noted in Fig. 10, where the phase angle between the flight and simulated oscillations is near zero.

Data acquisition rates for the 1-"g" stall and abrupt stall captive maneuvers of Figs. 9 and 10 were approximately 1.8 min and 3.4 min respectively, of wind tunnel time per second of flight time. The improved acquisition of the 1-"g" stall may be attributed to the reduced control deflection rates (see longitudinal stick). The data acquisition rate of Fig. 10 corresponds to that presented in Figs. 7 and 8, which also show high control deflection rates.

4.4 WIND-UP TURN TO STALL

An accelerated stall resulting from a wind-up turn maneuver is shown in Fig. 11. The maneuver is initiated with the aircraft in a 3.8-"g" (N_Z) banked turn at 0.75 Mach number. The near-4-"g" turn is maintained by increasing angle of attack (via longitudinal stick position) as Mach number decreases until maximum control surface and/or lift coefficient is reached. As experienced with previous high-AOA maneuvers an uncommanded wing-rock motion commences as aircraft angle of attack passes approximately 20 deg. The captive system is successful in simulating these motions although, for reasons adressed in Section 4.3, the phase angle is different.

The commanded motion ALPHA, THETA, and N_Y of Fig. 11 are in good agreement with flight. A high-"g" maneuver such as the wind-up turn normally results in a rapid bleed-off in Mach number for constant throttle settings. An example is the maneuver in Fig. 11 where Mach number decreases from 0.75 to 0.35 in 13 sec flight time. In captive testing the tunnel Mach number is maintained within ± 0.005 of the calculated Mach number at all times. The continuous wind tunnel Mach number adjustment was accomplished for the wind-up turn maneuver without delay in data acquisition. The data acquisition rate was approximately 3 min. tunnel time per second of flight time.

5.0 CONCLUDING REMARKS

As a result of the captive test experiment, the following conclusions and observations are noted:

1. Accurate simulation of complex high-angle-of-attack aircraft maneuvers may be obtained with captive testing as verified by wind tunnel/flight correlations.
2. The fabrication of remote control surfaces on small wind tunnel models (1/20 scale) is feasible, and the reliability and accuracy of these control surfaces are acceptable for captive testing.
3. Uncommanded motion (wing rock) near aircraft stall was simulated accurately with the captive system. The inherent inclusion of all aerodynamic nonlinear and hysteresis phenomena in captive testing is believed to be an important factor in perturbating this motion.
4. Wind tunnel time required for generating captive maneuvers ranged from 1.8 min to 3.5 min tunnel time per second of flight time.

REFERENCES

1. Milillo, J. R. "Post-Stall Testing of Aircraft with a Wind Tunnel Captive System." AEDC-TR-72-126 (AD751461), November 1972.

2. Butler, R. W. "Evaluation of a Wind Tunnel Technique to Determine Aircraft Departure Characteristics" AEDC-TR-73-183 (AD776317), March 1974.

3. Butler, R. W. "A Wind Tunnel Captive Aircraft Testing Technique." AEDC-TR-76-22 (AD-A023690), April 1976.

4. Test Facilities Handbook (Eleventh Edition). "Propulsion Wind Tunnel Facility, Vol. 5." Arnold Engineering Development Center, June 1979.

5. Abernethy, R. B. and Thompson, J. W., Jr. "Handbook — Uncertainty in Gas Turbine Measurements." AEDC-TR-73-5 (AD755356), February 1973.

6. Wilson, D. B. and Winters, C. P. "F-15A Approach-To-Stall/Stall/Post-Stall Evaluation." AFFTC-TR-75-32, January 1976.

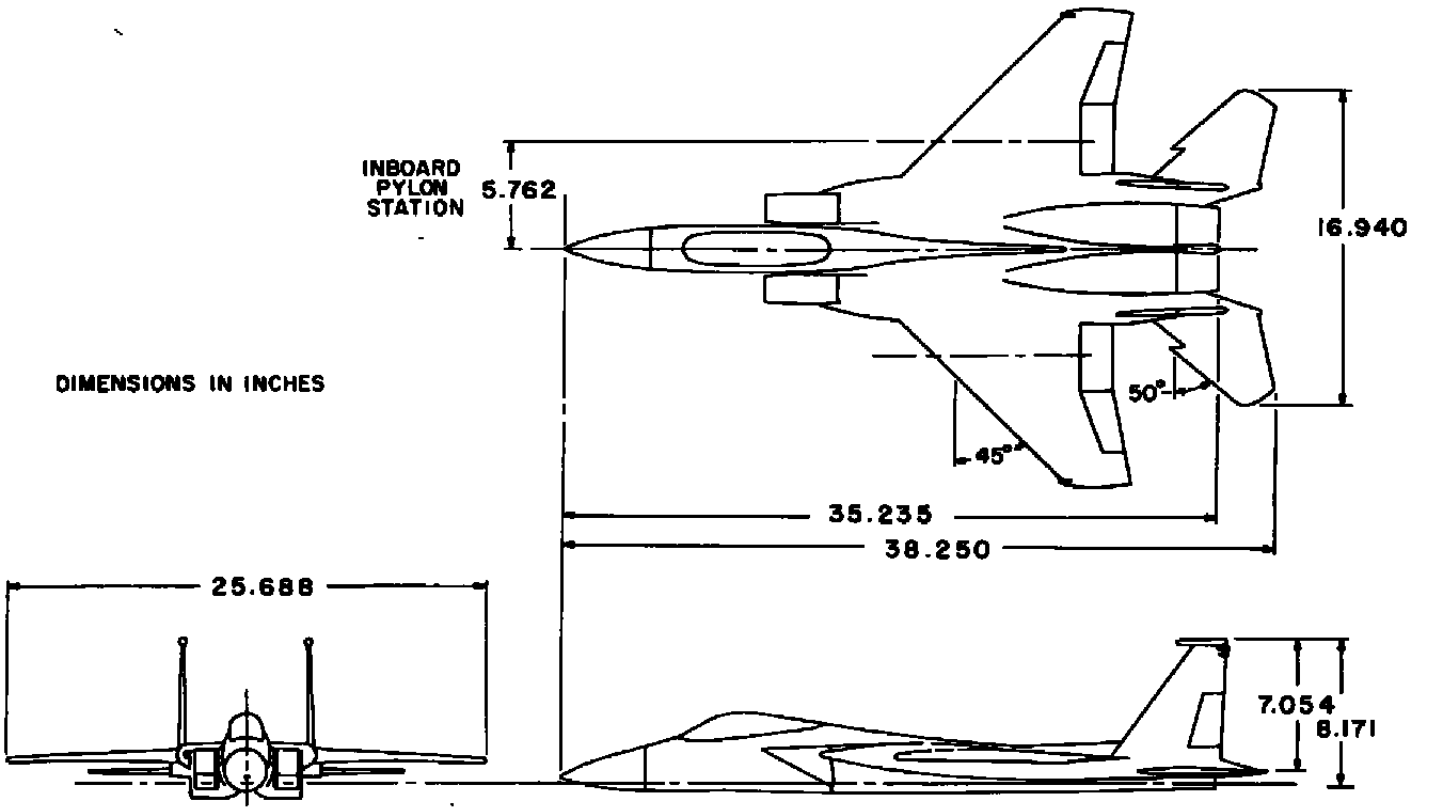

Figure 1. Aircraft model used in captive demonstration.

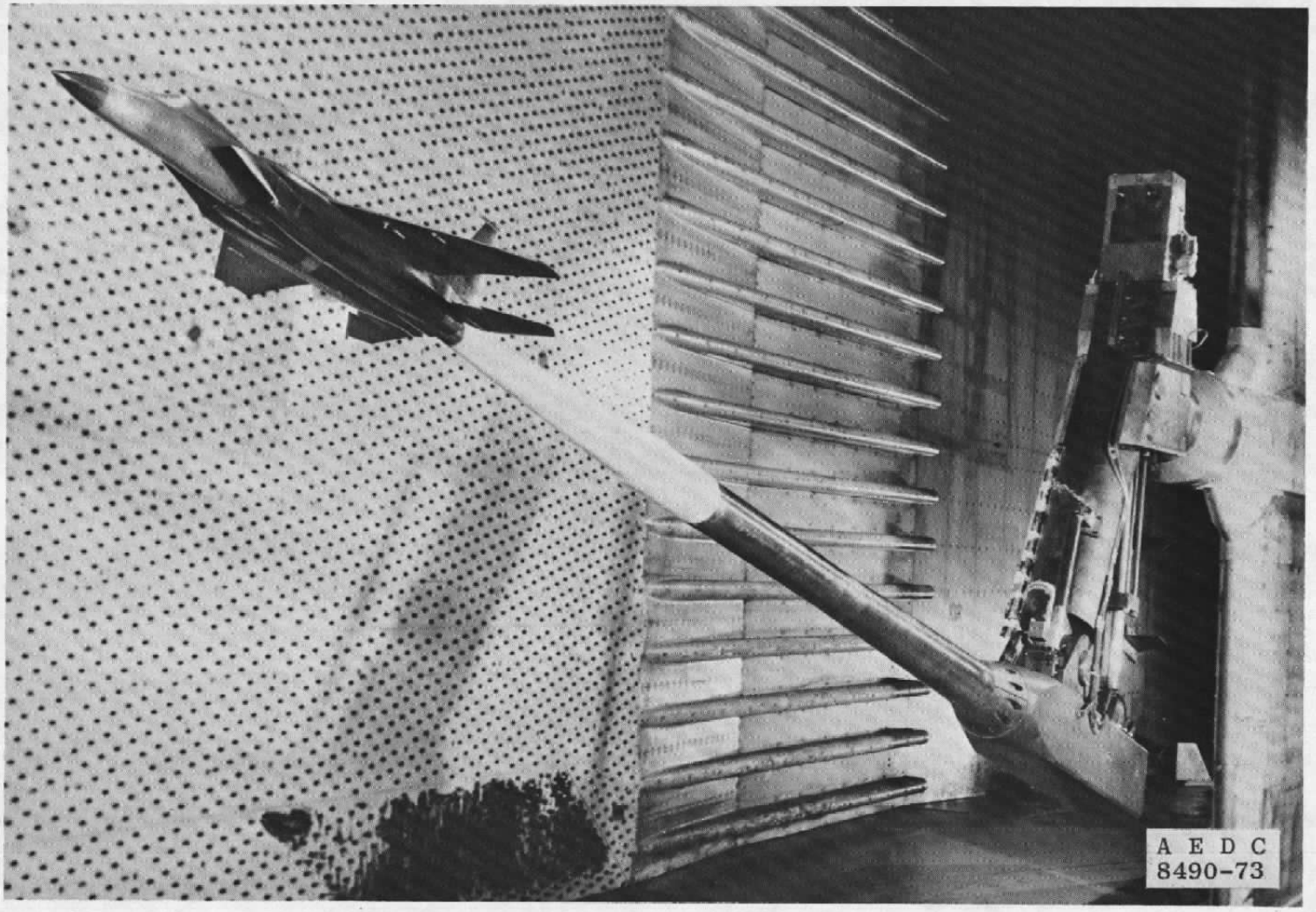

Figure 2. Aircraft model installed in Tunnel 16T test section.

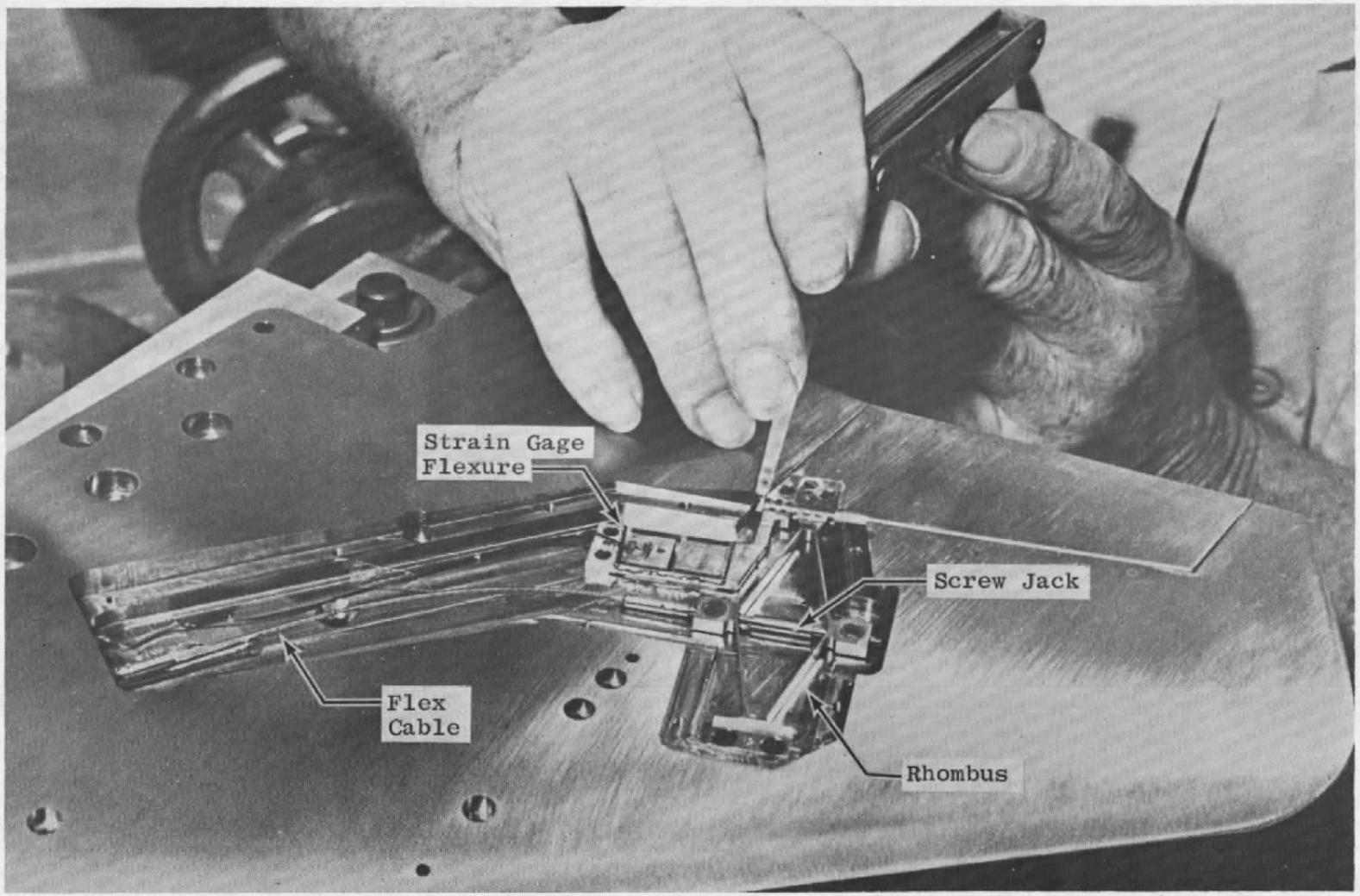

Figure 3. Aileron drive mechanism developed for captive model.

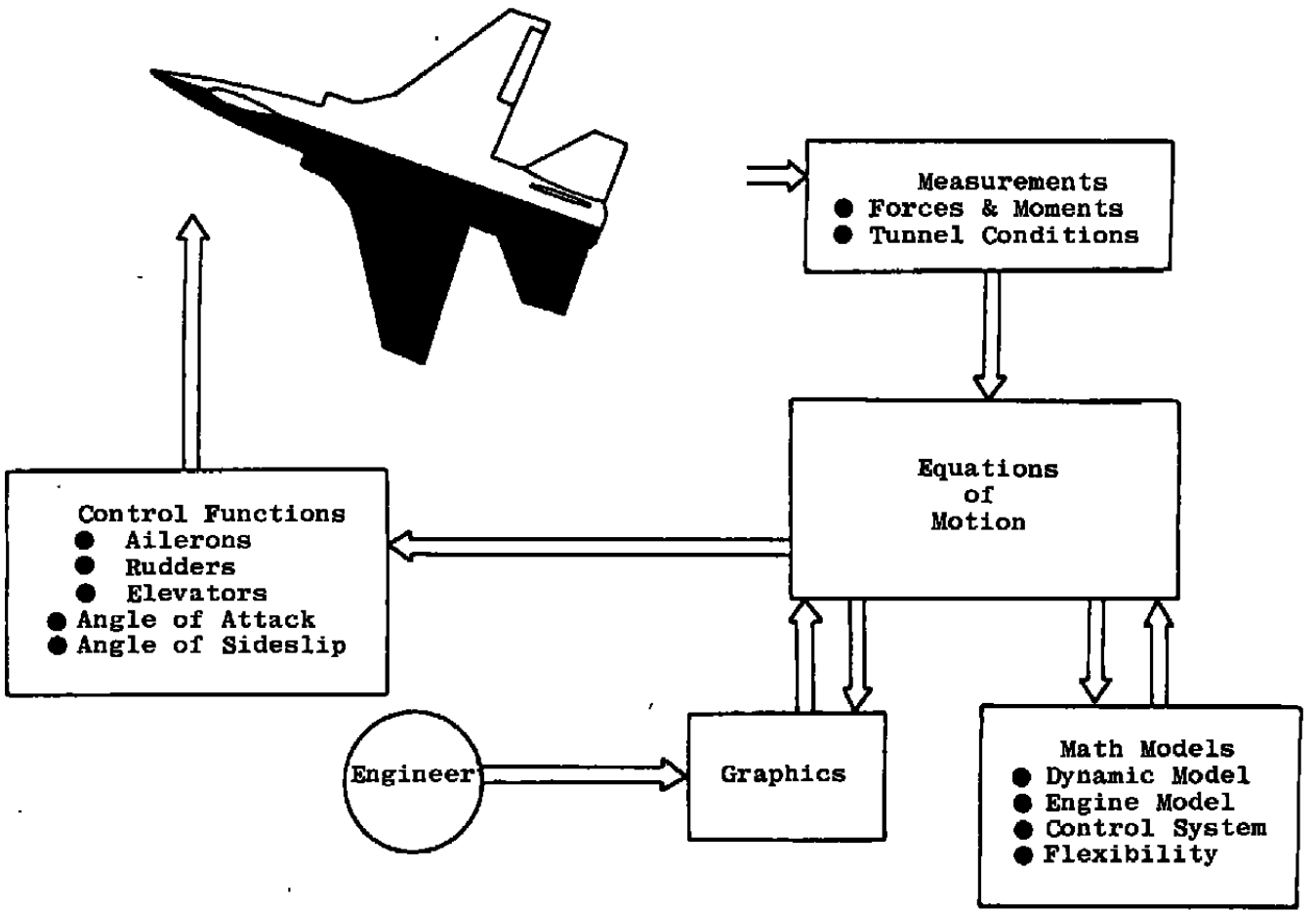

Figure 4. Captive closed loop data acquisition system.

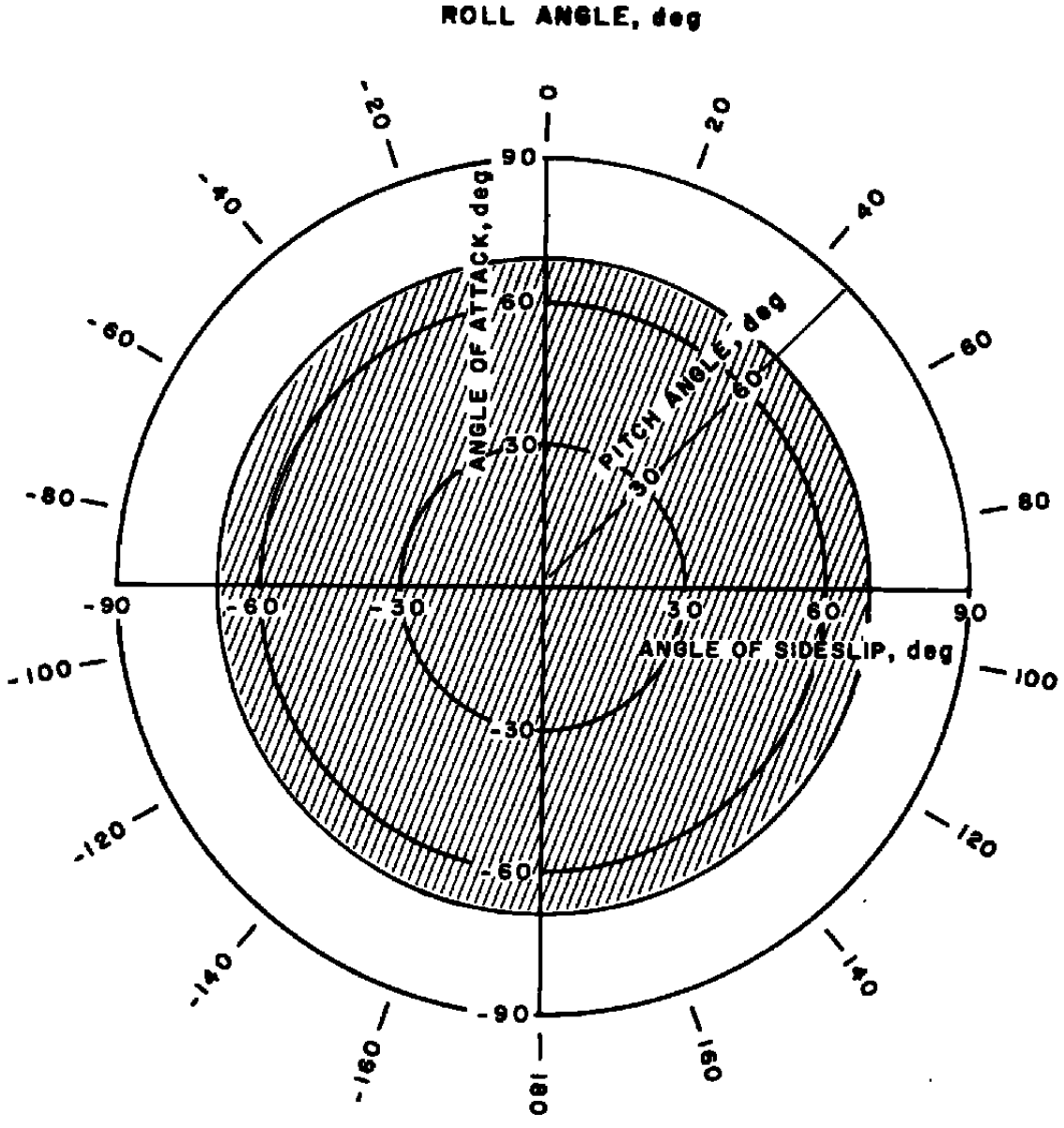

Figure 5. Tunnel 16T angle-of-attack and angle-of-sideslip capabilities.

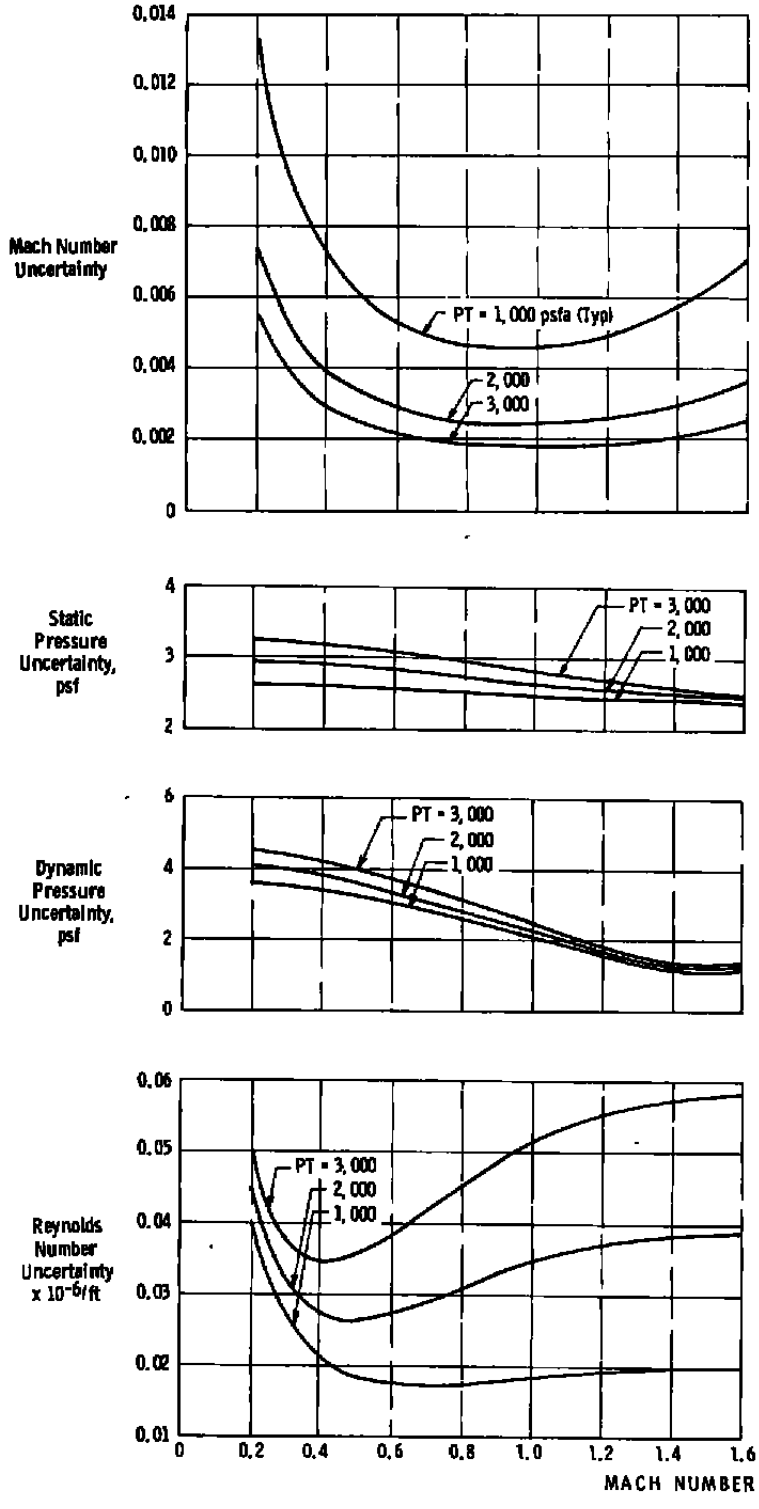

Figure 6. Estimated uncertainties in wind tunnel parameters.

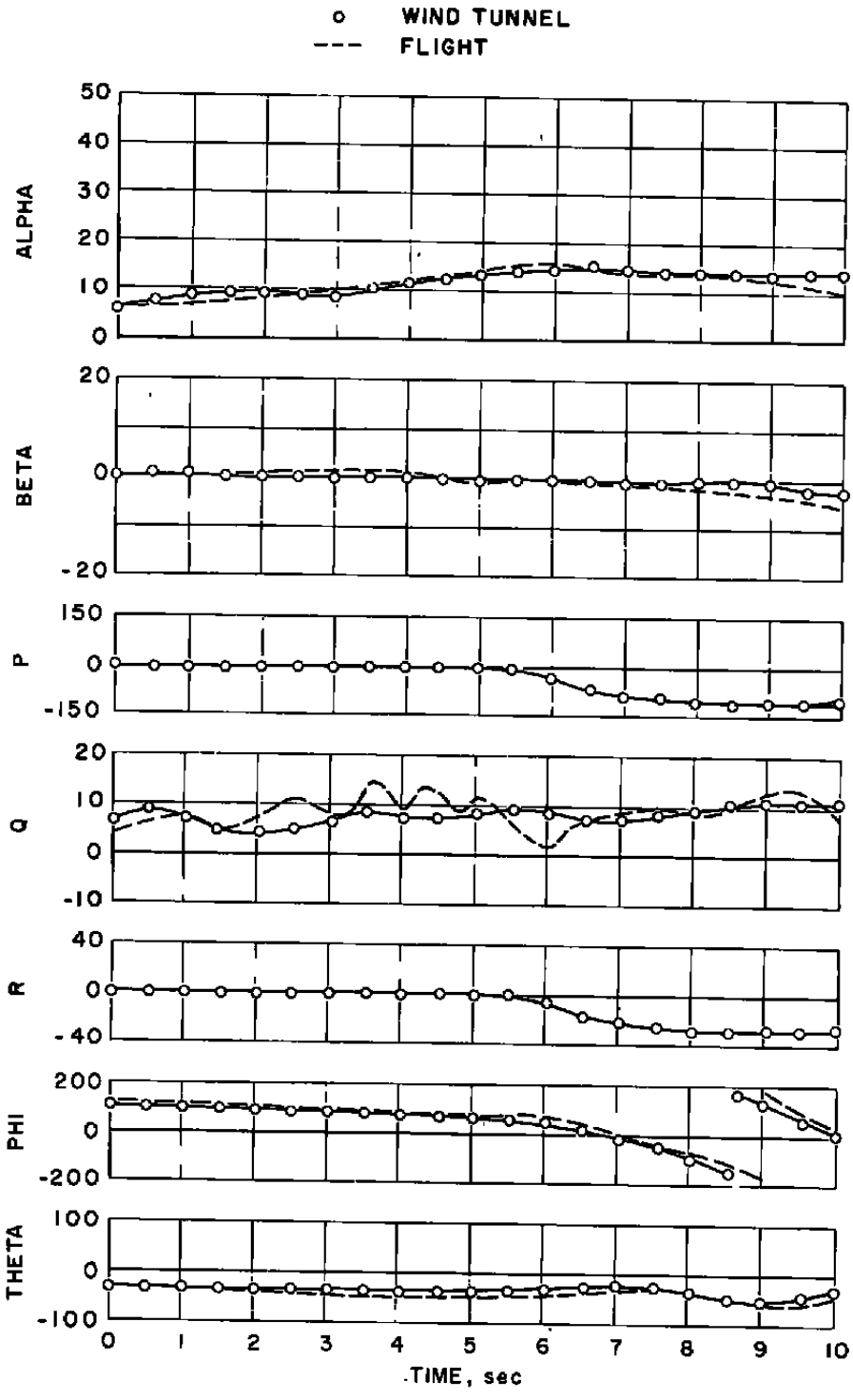

Figure 7. Full lateral stick roll maneuver.

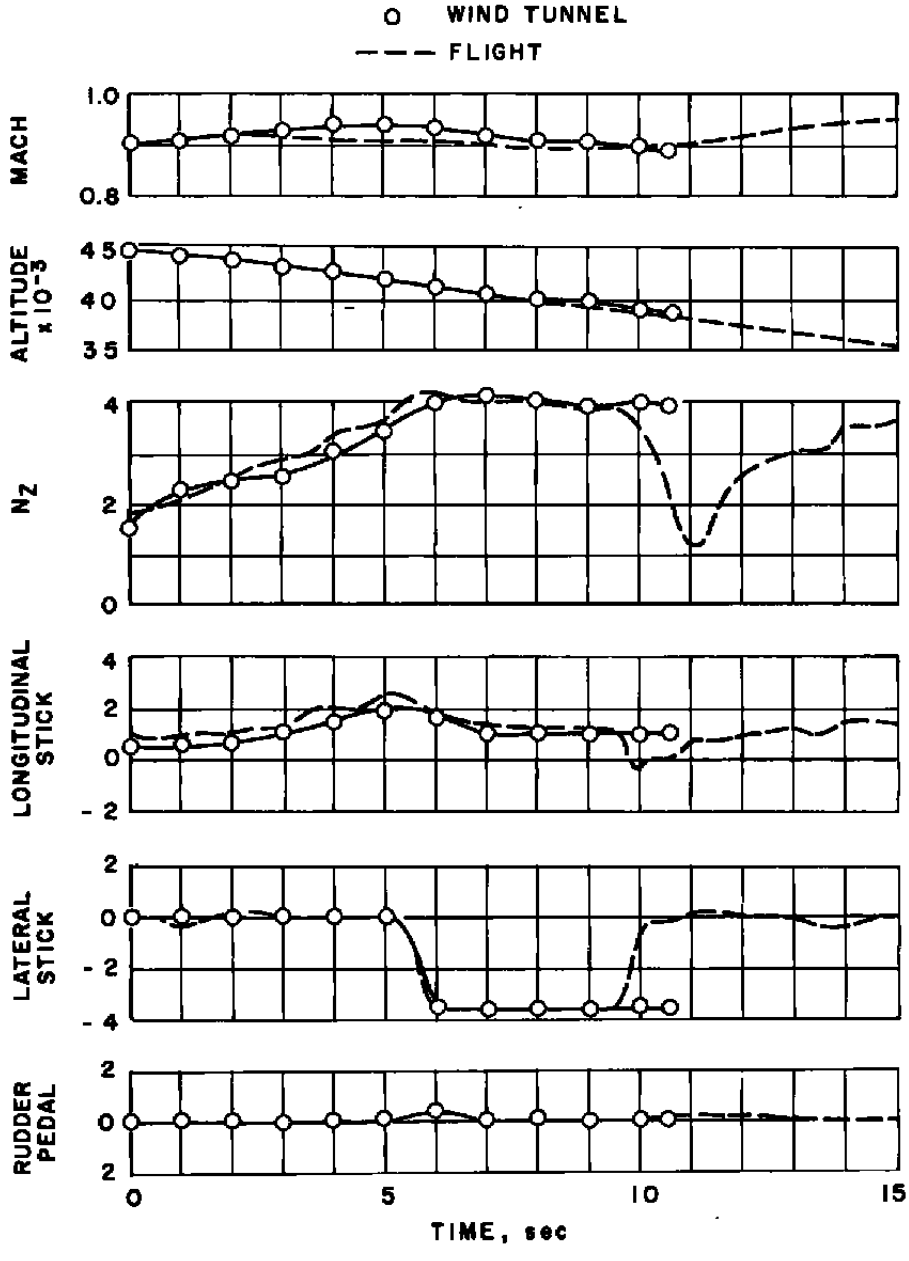

Figure 7. Concluded.

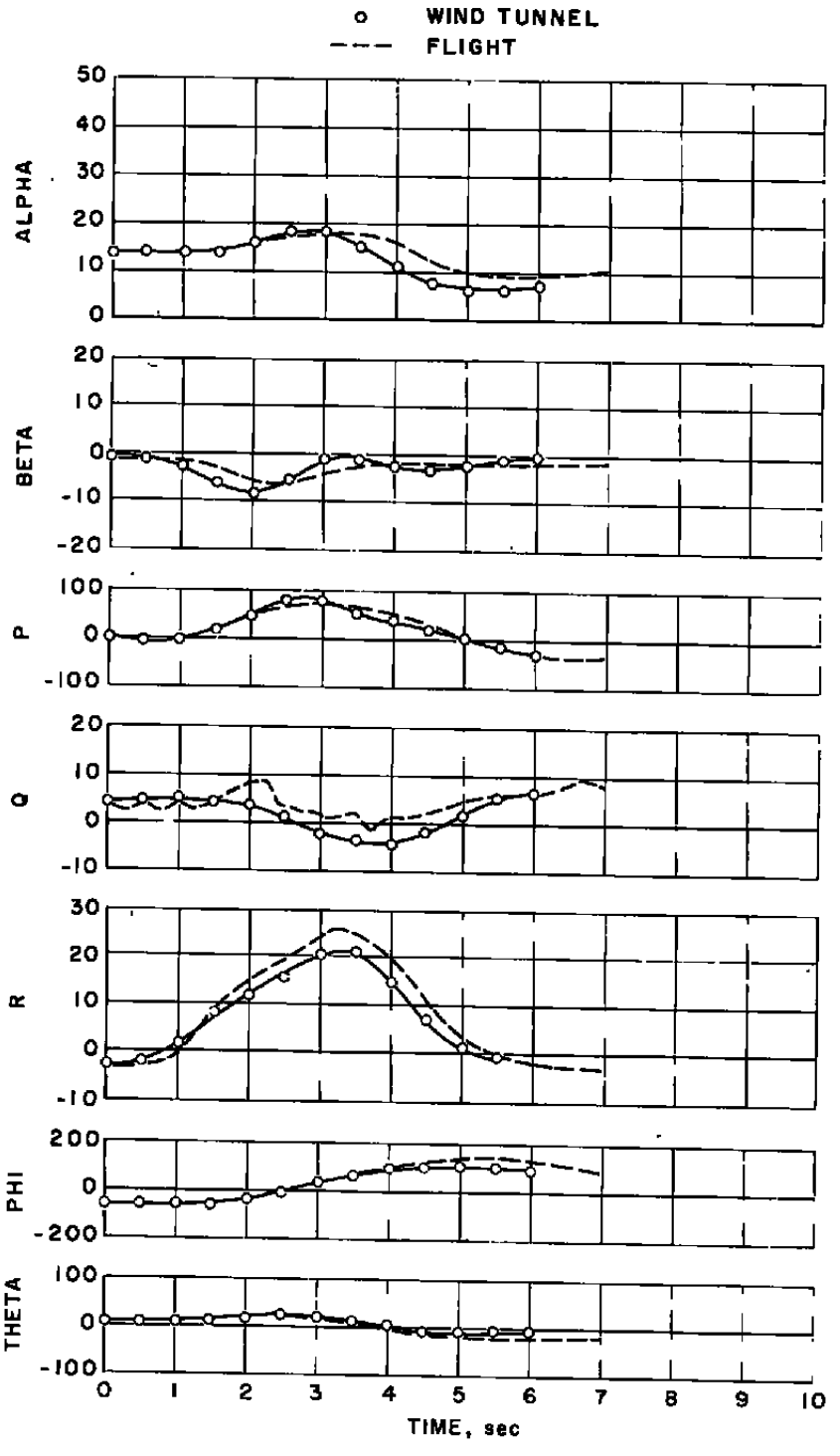

Figure 8. Full rudder pedal roll maneuver.

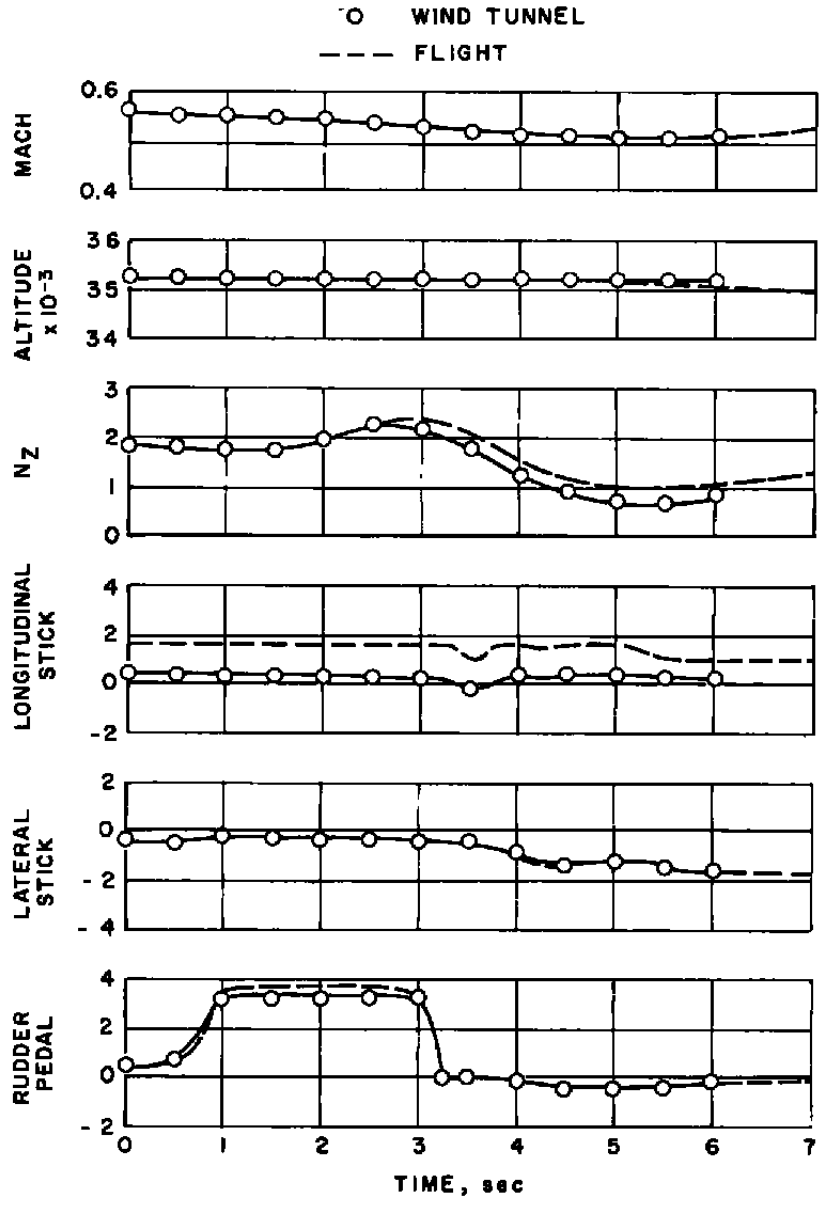

Figure 8. Concluded.

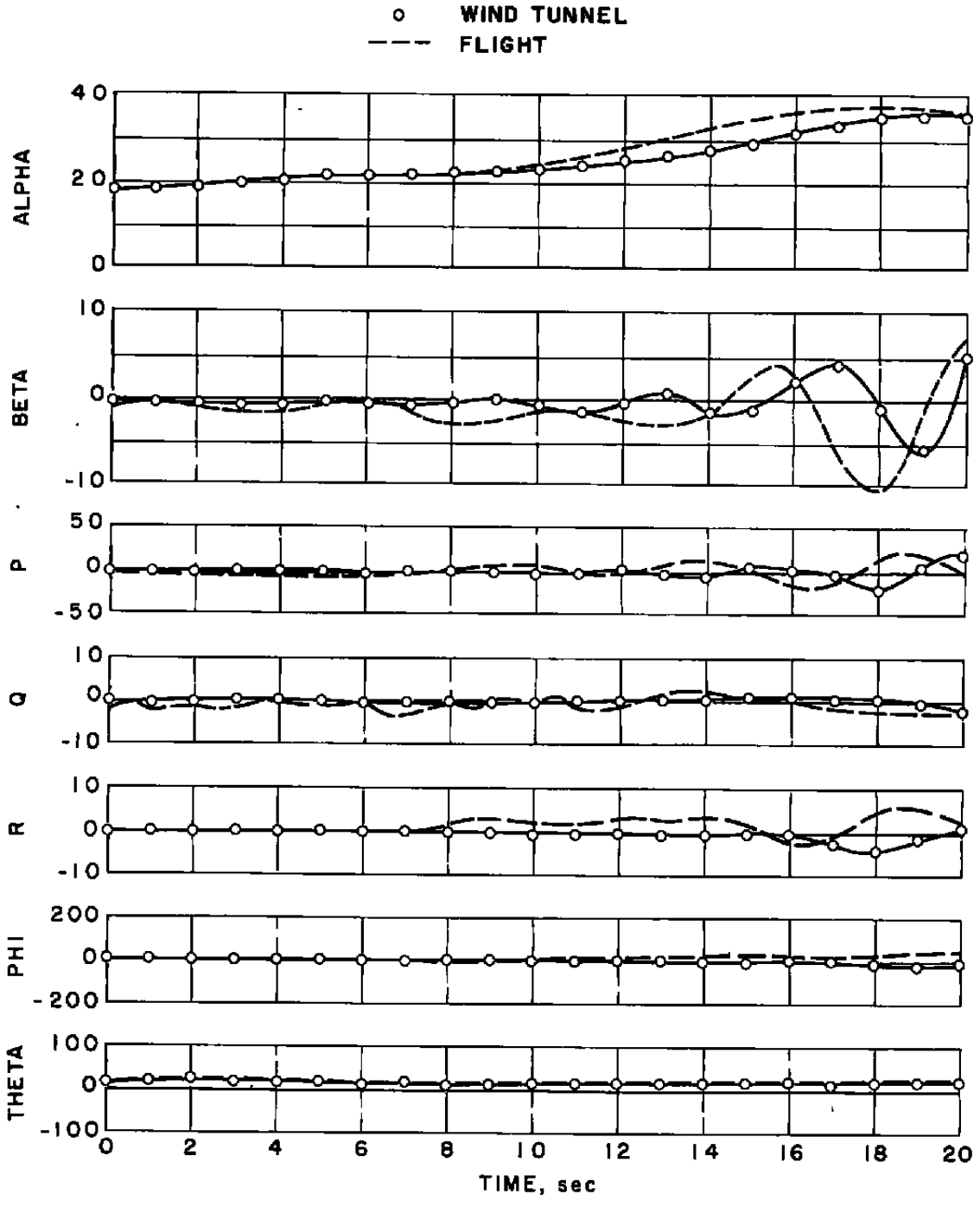

Figure 9. One-"g" stall maneuver.

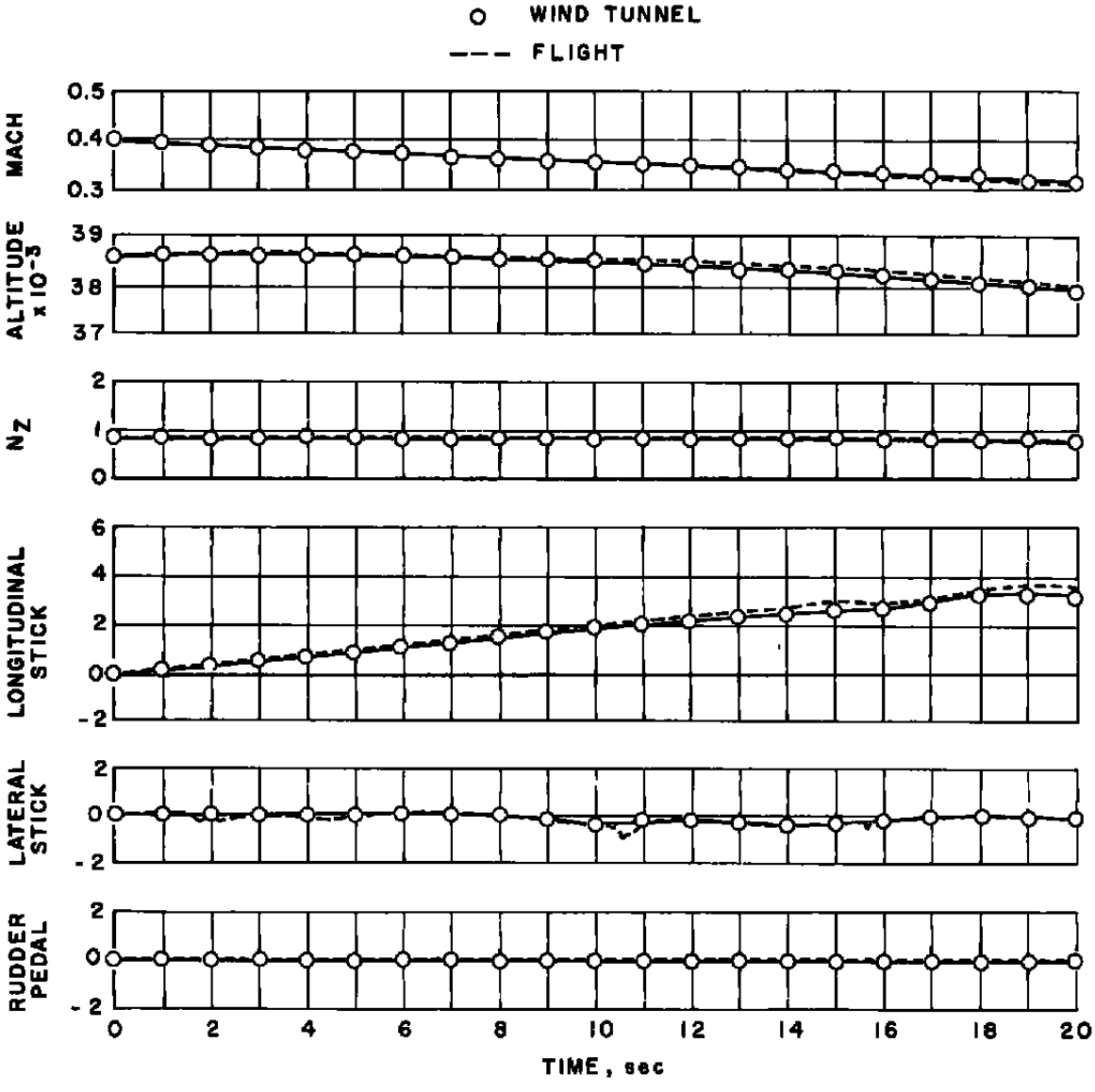

Figure 9. Concluded.

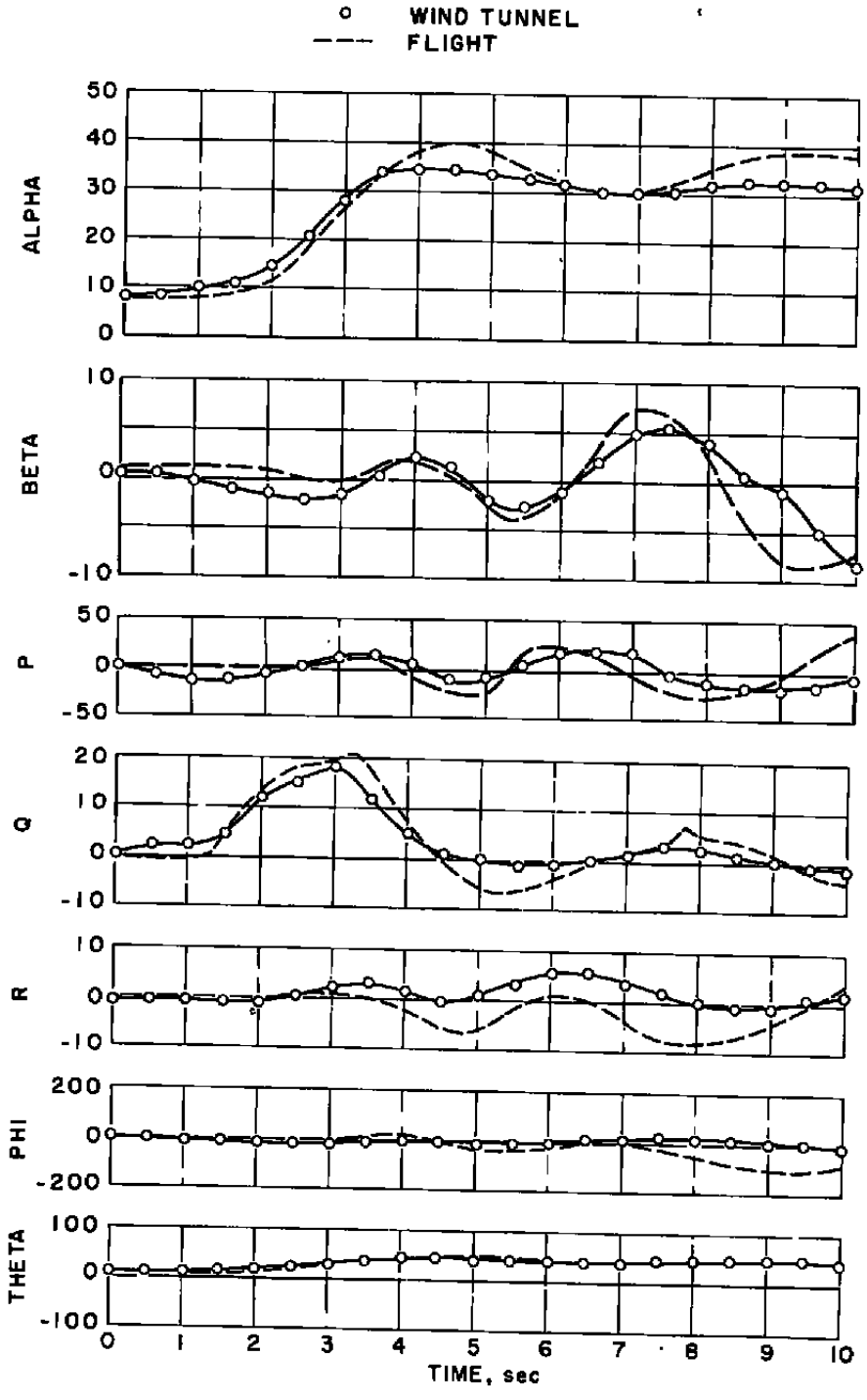

Figure 10. Abrupt stall maneuver.

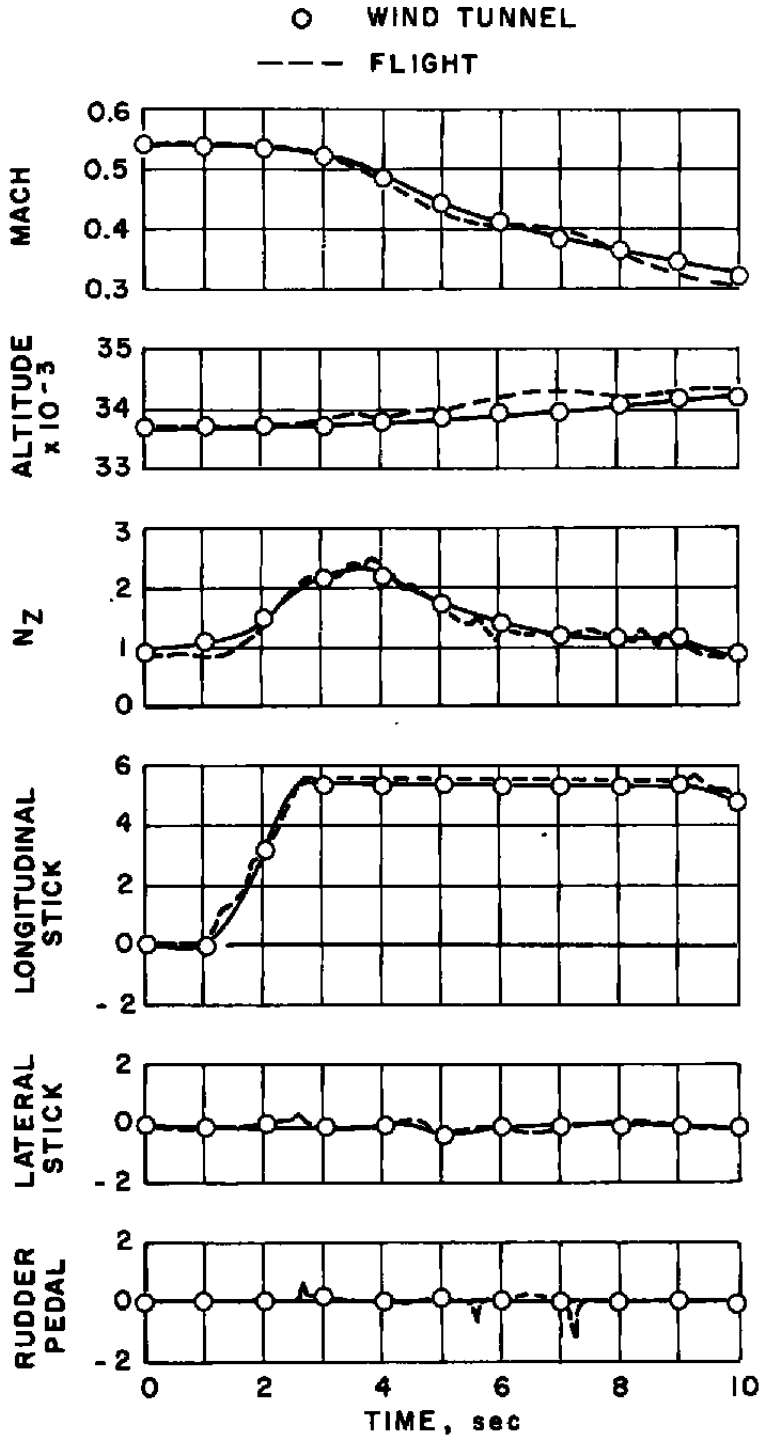

Figure 10. Concluded.

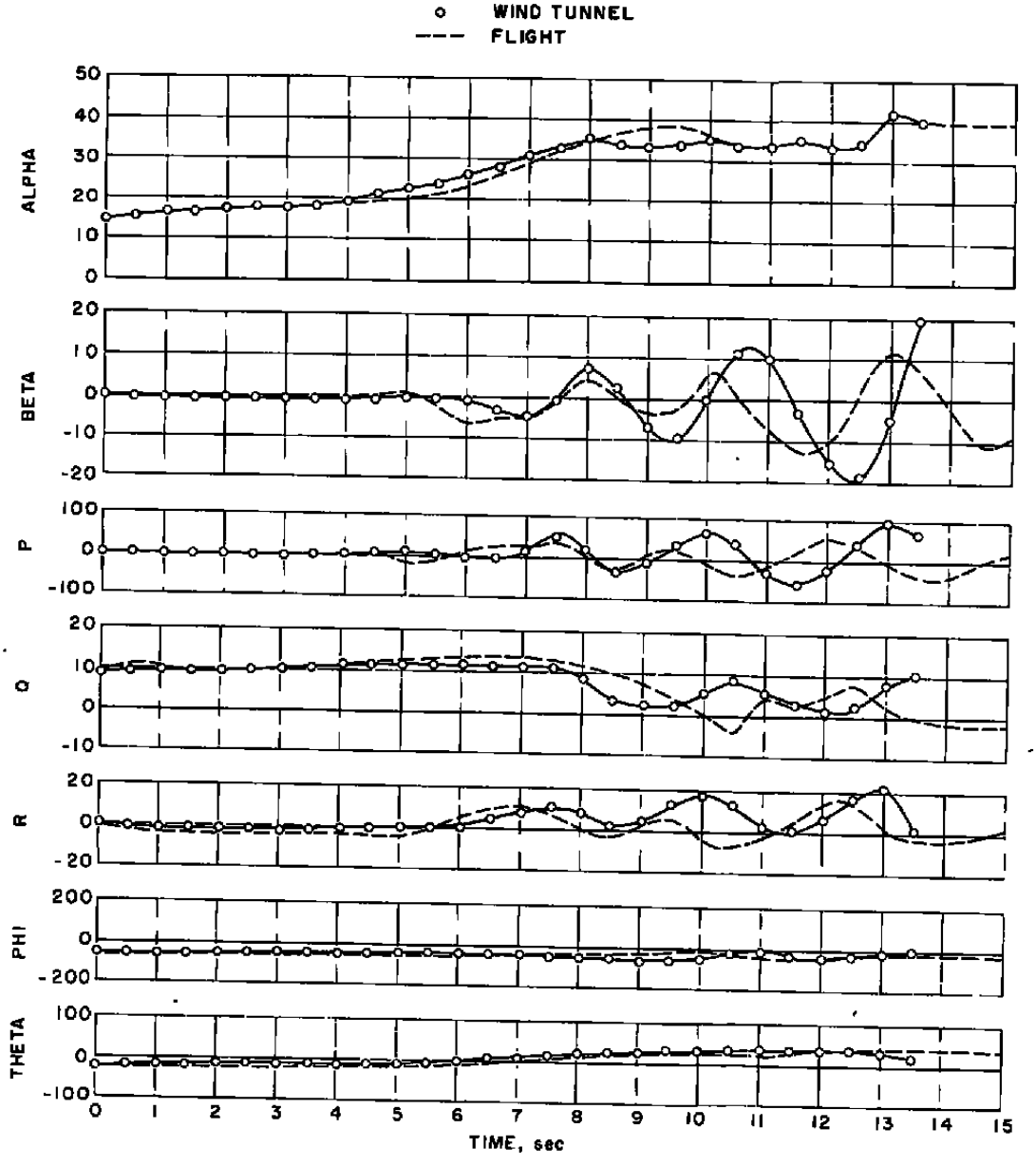

Figure 11. Wind-up turn maneuver.

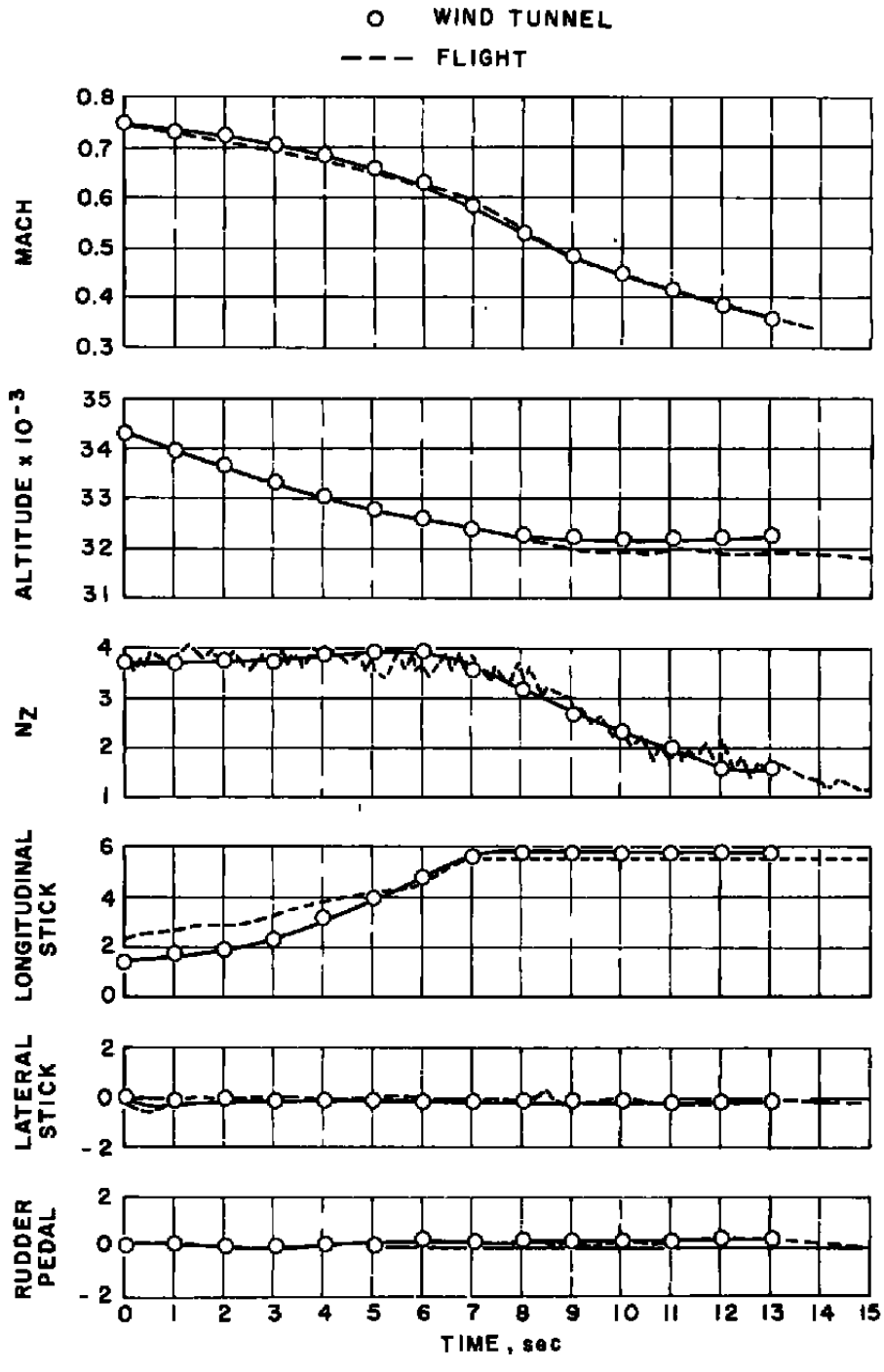

Figure 11. Concluded.

Table 1. Characteristics of Aircraft Simulated in Captive Testing

Maneuver	Weight, lb	cg, Percent $\bar{c}$	I_x, Slug-ft^2	I_y, Slug-ft^2	I_z, Slug-ft^2	I_{xz}, Slug-ft^2	Power
Lateral Stick Roll	33,500	27.4	22,400	196,100	211,600	-1,000	Military
Rudder Pedal Roll	32,900	28.2	22,200	192,700	208,200	0	Military
One-"g" Stall	35,400	28.5	24,300	192,000	209,600	0	Military
Abrupt Stall	38,900	26.9	28,900	196,300	218,400	0	Military
Wind-Up Turn	33,400	28.8	22,500	189,800	205,600	0	Military

APPENDIX A
EULER EQUATIONS OF MOTION

APPENDIX A
EULER EQUATIONS OF MOTION

The following equations were used in calculating the motion of the aircraft during captive testing.

$$\dot{p} = \frac{G_x}{I_x} + \frac{R_x}{I_x} + \frac{I_{xz}}{I_x}(\dot{r} + pq) + \frac{I_y - I_z}{I_x} qr$$

$$\dot{q} = \frac{G_y}{I_y} + \frac{R_y}{I_y} + \frac{I_{xz}}{I_y}(r^2 - p^2) + \frac{I_z - I_x}{I_y} rp$$

$$\dot{r} = \frac{G_z}{I_z} + \frac{R_z}{I_z} + \frac{I_{xz}}{I_z}(\dot{p} - qr) + \frac{I_x - I_y}{I_z} pq$$

$$\dot{u} = \frac{x}{m} + \frac{T_x}{m} + n_1 g - qw + rv$$

$$\dot{v} = \frac{y}{m} + n_2 g - ru + pw$$

$$\dot{w} = \frac{z}{m} + \frac{T_z}{m} + n_3 g + qv - pv$$

The aerodynamic forces and moments used in the simulation were as follows:

$$x = x(\alpha, \beta)$$

$$y = y(\alpha, \beta) + \rho\frac{V_\infty Sb}{4}(C_{Y_r} r + C_{y_{\dot\beta}}\dot{\beta})$$

$$z = z(\alpha, \beta)$$

$$G_x = G_x(\alpha, \beta) + \rho\frac{V_\infty Sb^2}{4} C\ell_p p + C\ell_r r + C\ell_{\dot\beta}\dot{\beta})$$

$$G_y = G_y(\alpha, \beta) + \rho\frac{V_\infty S\bar{c}^2}{4}(C_{m_q} q + C_{m_{\dot\alpha}}\dot{\alpha})$$

$$G_z = G_z(\alpha, \beta) + \rho\frac{V_\infty Sb^2}{4}(C_{n_r} r + C_{n_p} p + C_{n_{\dot\beta}}\dot{\beta})$$

where $x(\alpha, \beta)$, $y(\alpha, \beta)$, $z(\alpha, \beta)$, $G_x(\alpha, \beta)$, $G_y(\alpha, \beta)$, and $G_z(\alpha, \beta)$ are the aerodynamic static forces and moments generated in the wind tunnel.

APPENDIX B
SIMULATED FLIGHT CONTROL SYSTEM

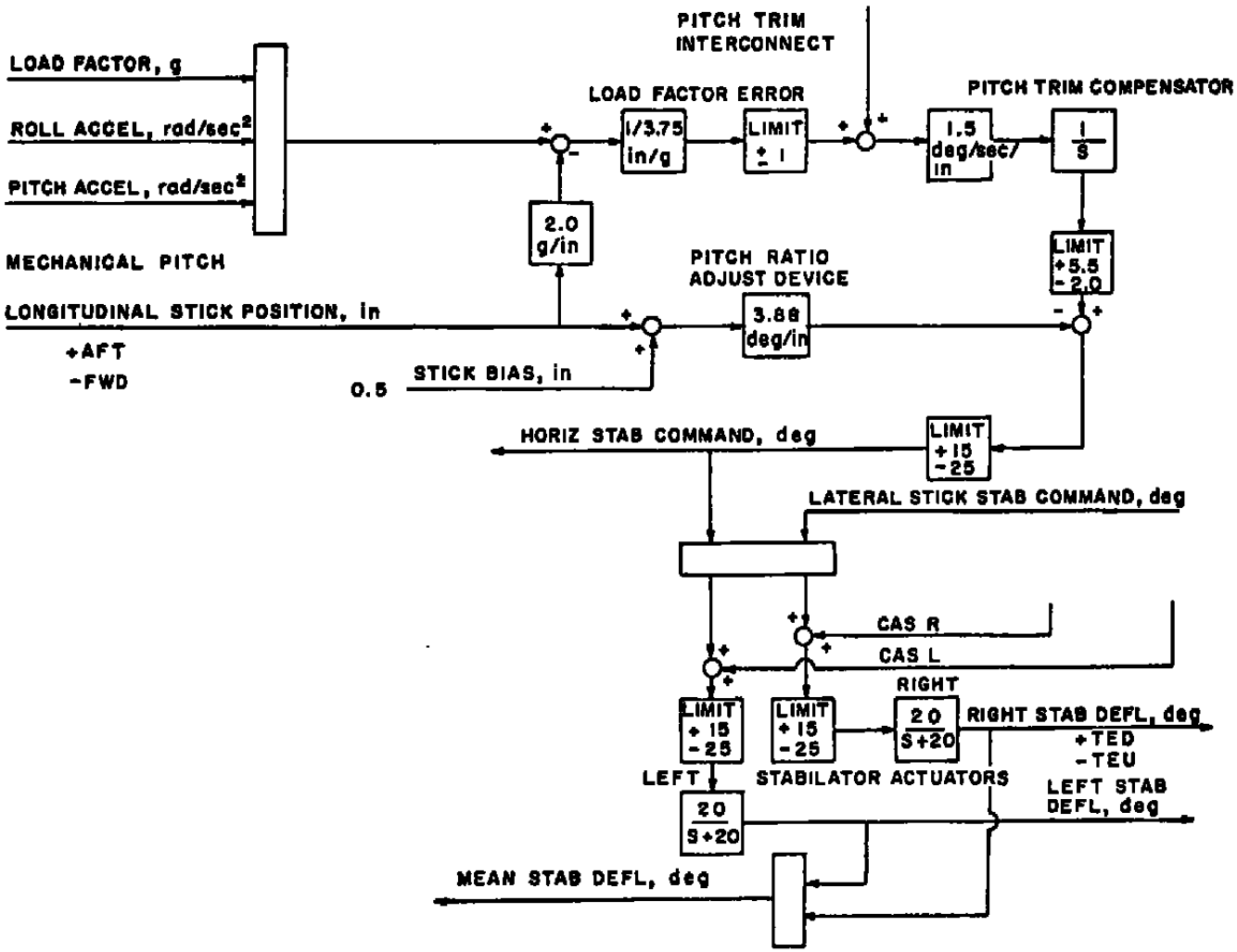

Figure B-1. Longitudinal control.

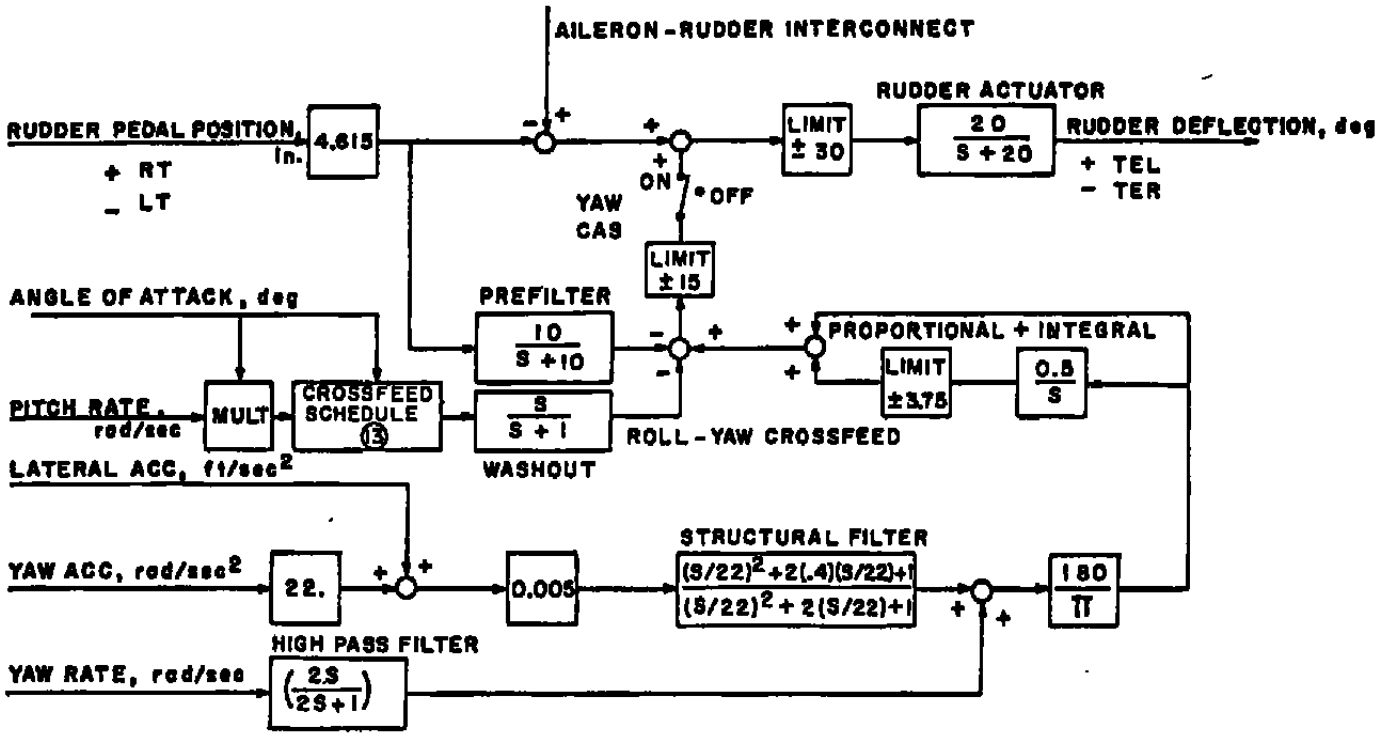

Figure B-2. Lateral control (rudder).

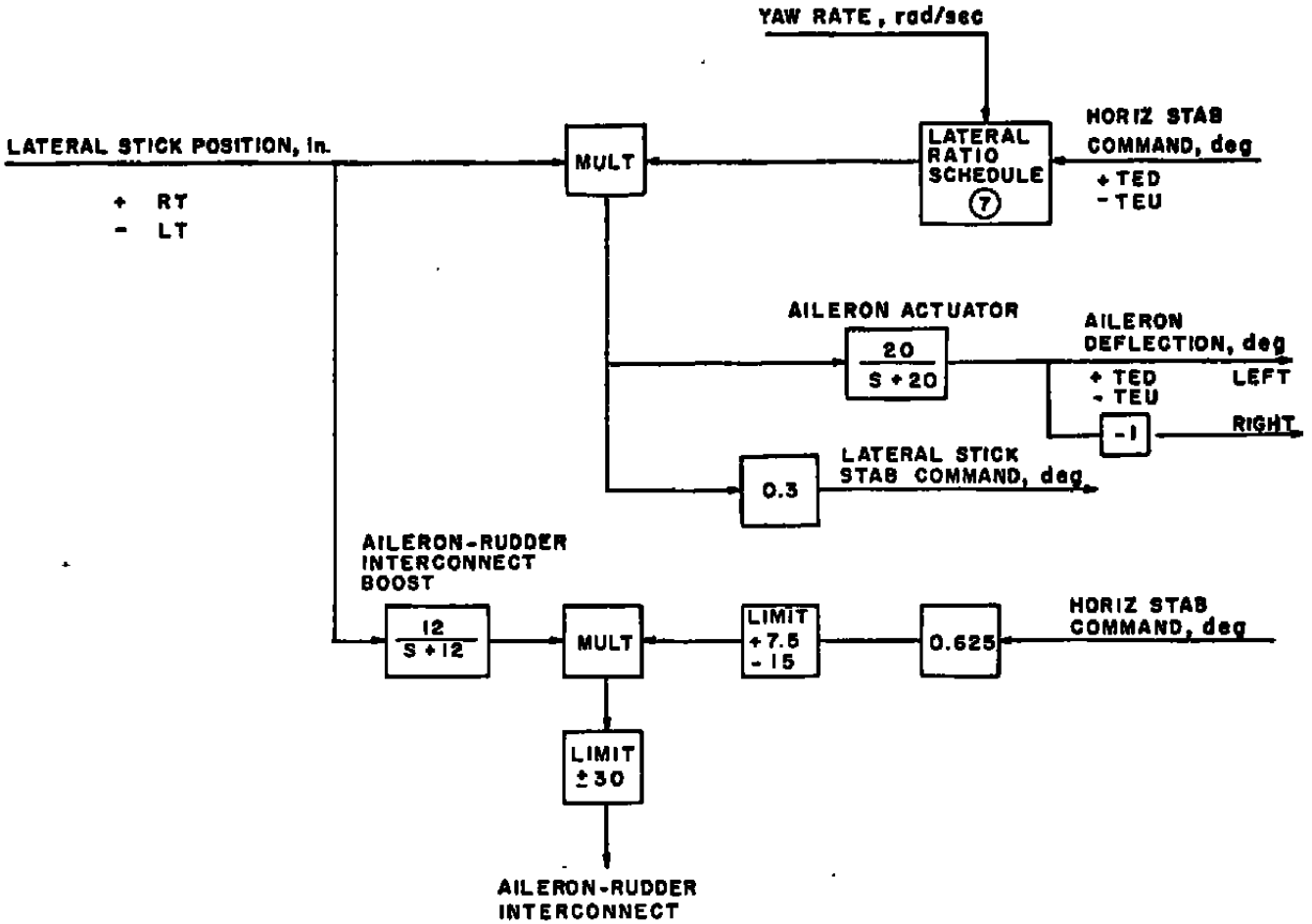

Figure B-3. Lateral control (aileron).

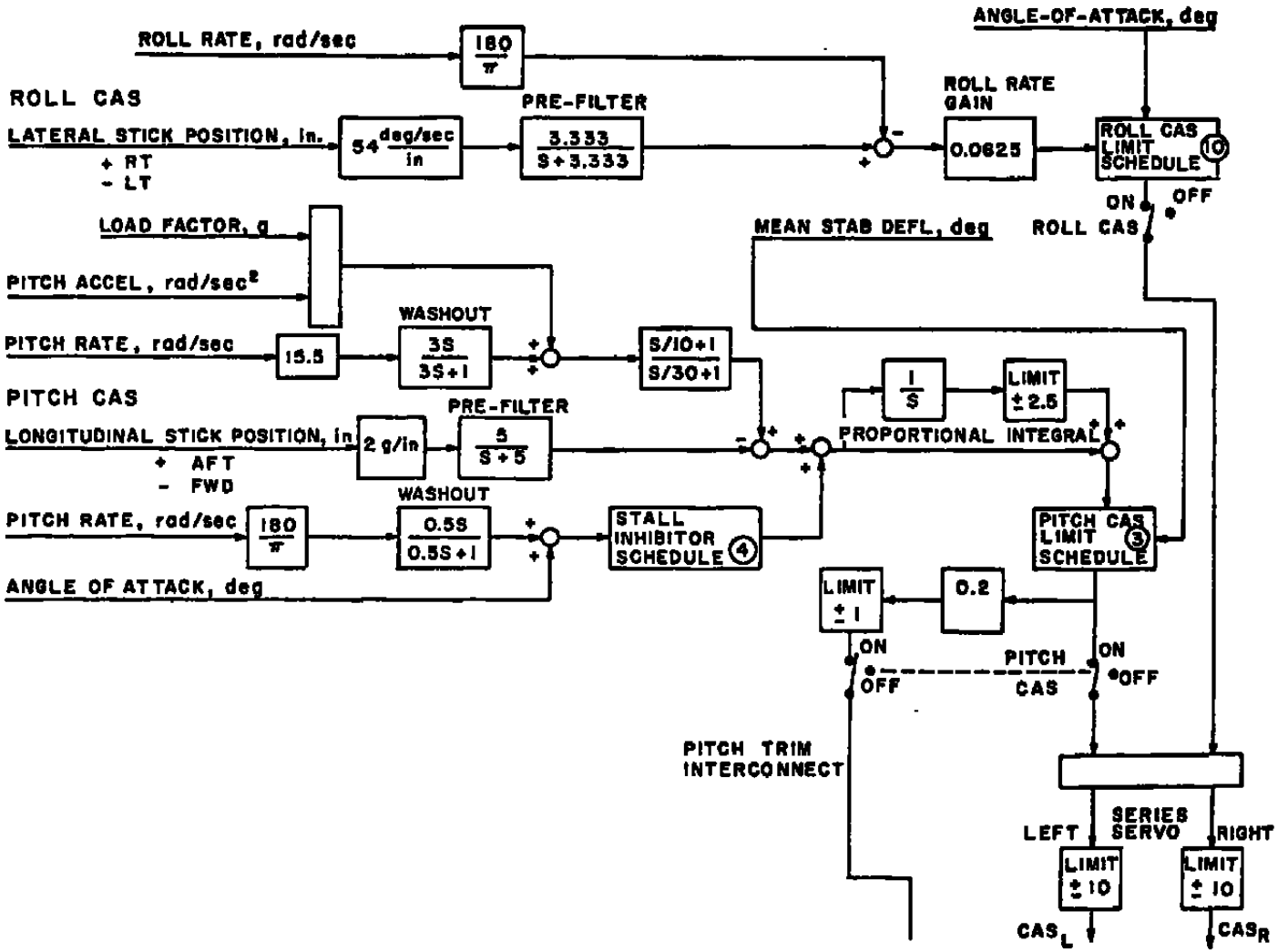

Figure B-4. CAS control system.

NOMENCLATURE

AOA	Angle of attack
b	Wing span, ft
C_ℓ	Rolling-moment coefficient, $M_x/q_\infty Sb$
C_{ℓ_p}	Dynamic damping derivative in roll, $\partial C_\ell/(\partial pb/2V_\infty)$
C_{ℓ_r}	Dynamic cross-derivative or rolling moment due to yawing, $\partial C_\ell/(\partial rb/2V_\infty)$
$C_{\ell\dot{\beta}}$	Lateral acceleration derivative in roll, $\partial C_\ell/(\partial \dot{\beta} b/2V_\infty)$
C_m	Pitching-moment coefficient, $M_y/q_\infty S\bar{c}$
C_{m_q}	Dynamic damping derivative in pitch, $\partial C_m/(q\bar{c}/2V_\infty)$
$C_{m_{\dot{\alpha}}}$	Longitudinal acceleration derivative in pitch, $\partial C_m/\partial\dot{\alpha}\bar{c}/2V_\infty)$
C_n	Yawing-moment coefficient, $M_z/q_\infty Sb$
C_{n_p}	Dynamic cross-derivative of yawing moment due to rolling, $\partial C_n/(\partial pb/2V_\infty)$
C_{n_r}	Dynamic damping derivative in yaw, $\partial C_n/(\partial rb/2V_\infty)$
$C_{n\dot{\beta}}$	Lateral acceleration derivative in yaw, $\partial C_n/(\partial \dot{\beta} b/2V_\infty)$
C_Y	Side-force coefficient, $F_Y/q_\infty S$
C_{Y_r}	Dynamic derivative of side force due to yawing, $\partial C_Y/(\partial rb/2V_\infty)$
$C_{Y\dot{\beta}}$	Lateral acceleration derivative in side force, $\partial C_Y/(\partial \dot{\beta} b/2V_\infty)$
$\bar{c}$	Mean geometric chord, ft
cg	Aircraft center of gravity
F_Y	Side force, lb
g	Acceleration due to gravity, ft/sec^2
G_x, G_y, G_z	Components of the aerodynamic moments about the X_B, Y_B, and Z_B axes, respectively, ft-lb
I_x, I_y, I_z	Moments of inertia about X_B, Y_B, and Z_B axes, respectively, slug-ft^2

I_{xz}	Product of inertia, slug-ft^2
M_x	Rolling moment, ft-lb
M_y	Pitching moment, ft-lb
M_z	Yawing moment, ft-lb
m	Aircraft mass slugs
N_Z	Load factor
n_1,n_2,n_3	Direction cosines of body axis relative to earth axis
PT	Tunnel total pressure, lb/ft^2
p,q,r	Aircraft roll, pitch, and yaw rates about the X_B, Y_B, and Z_B axes, respectively, deg/sec
q_∞	Dynamic pressure, lb/ft^2
R_x,R_y,R_z	Moment contributions from engine thrust about the X_B, Y_B, and Z_B axes, respectively, ft-lb
S	Wing area, ft^2
T_x,T_z	Components of engine thrust along the X_B and Z_B axes, respectively, ft/sec
u,v,w	Linear velocity components along the X_B, Y_B, and Z_B axes, respectively, ft/sec
V_∞	Free-stream velocity, $(u^2 + v^2 + w^2)^{1/2}$, ft/sec
X_B,Y_B,Z_B	Right-hand body-axis Cartesian coordinates, X positive forward
x,y,z	Components of the aerodynamic forces along the X_B, Y_B, and Z_B axes, respectively, lb
α	Angle of attack, $\tan^{-1} w/u$, deg or rad
β	Angle of sideslip, $\sin^{-1} v/V_\infty$, deg or rad
ϱ	Simulated air density, slugs/ft^2
NOTE:	Dot over symbol indicates derivative with respect to time.